JOURNAL OF CATALYSIS 146, 257–267 (1994)

Methylamine Synthesis over Solid Acid Catalysts: Microcalorimetric and Infrared Spectroscopic Studies of Adsorbed Species

D. T. Chen,*[,1] L. Zhang,*[,2] Chen Yi,† and J. A. Dumesic,*[,3]

*Department of Chemical Engineering, University of Wisconsin, Madison, Wisconsin 53706; and †Chemistry Department, Nanjing University, Nanjing, China

Received July 22, 1993; revised October 13, 1993

Microcalorimetry was used to determine the differential enthalpy changes of adsorption versus coverage on H–ZSM-5 and H–mordenite of reactants and products of methylamine synthesis. The enthalpy changes of adsorption of dimethylether, ammonia, monomethylamine, and dimethylamine on Brønsted acid sites vary linearly from −90 to −250 kJ/mol with the gaseous proton affinities of these basic molecules. The enthalpy changes of adsorption of water and methanol vary from −60 to −90 kJ/mol. *In situ* infrared spectroscopy indicates that methoxyl species are present on the catalyst in flowing methanol at temperatures near 600 K; however, adsorbed ammonia and methylamines are associated with the Brønsted acid sites in gas mixtures of methanol and ammonia typically used for methylamine synthesis at these temperatures. These results suggest that dimethylether formation from methanol may occur through surface methoxyl species, while methylamine synthesis most likely involves adsorbed ammonium cations.

INTRODUCTION

The synthesis of aliphatic amines has attracted interest in recent years due to the increasing demand for amine compounds in the pharmaceutical and agricultural industries (1). Lower aliphatic amines are important intermediates in the synthesis of herbicides, pesticides, dyes, and pharmaceuticals that contain amino groups (2). The primary method of methylamine synthesis is the amination of methanol with ammonia over solid acid catalysts (3), with approximately 270 million lb. of methylamines produced per year in the United States (1).

In addition to its industrial significance, methylamine synthesis may be a useful probe of catalyst acidity. The reaction displays both activity and selectivity patterns, since the products consist of mono-, di-, and trimethylamine, water, and dimethylether. Moreover, ammonia and methylamines have been used as probe molecules for adsorption on the Brønsted and Lewis acid sites of oxides (4) and acid zeolites (5–9). In addition, alcohol adsorption on acid sites leads to the formation of surface alkoxyl species that may be important reaction intermediates (10, 11). Accordingly, studies of the catalytic cycles involved in methylamine synthesis reactions may offer insight into the acidic properties of the catalyst through interpretation of the observed kinetic behavior.

The nature of adsorbed species in methylamine synthesis will be addressed in this paper. Microcalorimetry is employed to measure the enthalpy changes of adsorption on the catalyst surface of various reactants and products involved in methylamine synthesis, while infrared spectroscopy is used to identify the nature of adsorbed species. A subsequent publication presents results from reaction kinetics studies (12). Our strategy in these studies is to employ a variety of experimental techniques to elucidate the catalytic cycles involved in methylamine synthesis. The microcalorimetric and IR spectroscopic results of the present paper provide important quantitative information about the surface thermodynamic and chemical aspects of these cycles that will be employed in our subsequent analyses of the kinetic aspects of these cycles (12).

EXPERIMENTAL

Two acidic zeolites were used for adsorption studies, H–ZSM-5 and H–mordenite. The H–ZSM-5 sample was provided by W. Haag of Mobil Corporation and had a Si/Al ratio of 35. The H–mordenite was obtained from the Conteka Corporation and had a Si/Al ratio of 13.

The microcalorimetry apparatus employed in these studies has been described previously (13). Catalyst samples (100–500 mg) were loaded in powder form into vacuum cells, followed by evacuation ($\sim 10^{-5}$ Torr) for 1 h at 473 K, 1 h at 573 K, and 1 h at 723 K. Oxygen was admitted into the cells at a pressure of 730 Torr and a temperature of 723 K, and the catalyst was calcined for

[1] Current address: 3M Corporation, St. Paul, MN 55144.

[2] Current address: McGill University, Chemistry Department, Montreal, Canada.

[3] To whom correspondence should be addressed.

0021-9517/94 $6.00

4 h, during which oxygen in the cells was periodically evacuated and replenished. Samples were subsequently degassed at 723 K for 1.5 h. The calorimeter block (typically at 473 or 423 K) was then raised around the cells, and the samples were evacuated overnight at this temperature. The final pressure was typically 5×10^{-5} Torr with a leak rate of 10^{-6} Torr/s into the system.

Differential enthalpy changes of adsorption versus adsorbate coverage were obtained by consecutive adsorption of 1–3 μmol doses of ammonia, monomethylamine (MMA), dimethylamine (DMA), trimethylamine (TMA), methanol, dimethylether (DME), and water. Coadsorption experiments were also conducted in which either methanol or DME was first adsorbed on H–mordenite at 473 K, the catalyst temperature was raised to 548 K, the catalyst was degassed at 5×10^{-5} Torr overnight, and ammonia was then adsorbed at 473 K.

The Si/Al ratios of ZSM-5 and mordenite samples studied in this work correspond to approximately 460 and 1200 μmol/g of Al atoms, respectively, The ZSM-5 sample also contained approximately 70 μmol/g of sodium cations. Therefore, the maximum numbers of acid sites that can be expected for these ZSM-5 and mordenite samples are 390 and 1200 μmol/g. It is important to note, however, that the microcalimetric measurements of this study for various bases on a given zeolite were conducted sequentially on the same sample, with calcination at 723 K between experiments. It is possible that small amounts of strongly adsorbed bases may not have been removed completely during these calcination treatments, thereby blocking acid sites during subsequent experiments. Therefore, we have not attempted to interpret apparent changes in the numbers of adsorption sites for the various bases on a given zeolite.

Infrared spectra were recorded using a Nicolet Model 7199C Fourier transform infrared spectrometer. Adsorption and *in situ* reaction experiments were conducted using a 2.5 cm diameter, self-supporting H–ZSM-5 wafer in a stainless-steel cell equipped with CaF_2 windows. The sample was pretreated in flowing O_2 (100 cm_3/min) for 4 h prior to each experiment. Methanol, ammonia, and monomethylamine were each adsorbed at 298 K and vapor pressures of approximately 10, 7, and 40 Torr, respectively. Helium was then passed at 100 cm^3/s through the IR cell, and spectra were taken after the initial helium purge at room temperature and at various temperatures typically up to 623 K.

In situ IR studies were performed with the H–ZSM-5 catalyst in a flowing gas mixture of 10 Torr methanol, 7 Torr ammonia, and 743 Torr helium. This gas mixture was passed at a flowrate of 500 cm^3/min over the catalyst at room temperature. The catalyst temperature was then raised to 673 K, with infrared spectra collected at various temperatures during heating.

RESULTS

Microcalorimetry of Amines

The differential enthalpy changes of adsorption versus adsorbate coverage for ammonia, monomethylamine, dimethylamine, and trimethylamine on H–ZSM-5 are shown in Fig. 1. Plots of the corresponding differential enthalpy changes of adsorption versus adsorbate coverage on H–mordenite are presented in Fig. 2.

Ammonia Adsorption

The differential enthalpy change of adsorption versus coverage for ammonia on H–ZSM-5 at 473 K shows two plateaus corresponding to adsorption on strong and weak sites. The strong sites have an average enthalpy change of adsorption of -151 ± 11 kJ/mol, and the weak sites adsorb ammonia at -69 ± 3 kJ/mol. There are approximately 300 μmol/g of strong sites. The behavior for ammonia adsorption on H–mordenite at 473 K is similar to that for H–ZSM-5. The major difference between these two samples is that mordenite has a small number of very strong sites, in addition to the large number of strong sites comprising the broad plateau in the plot of adsorption enthalpy change versus coverage. The initial region of this plot for H–mordenite, involving the very strong sites, has also been measured for pyridine adsorption (14). The total number of strong adsorption sites is approximately 900 μmol/g, with an average enthalpy change of ammonia adsorption equal to -158 ± 8 kJ/mol. The weak sites adsorb ammonia at -72 ± 2 kJ/mol.

Monomethylamine Adsorption

The differential enthalpy change versus coverage for monomethylamine adsorption on H–ZSM-5 at 473 K varies from -230 to -180 kJ/mol as the coverage increases to 250 μmol/g. The average enthalpy change of adsorption for these sites is -204 ± 22 kJ/mol. Weaker sites with differential enthalpy changes of MMA adsorption equal to -98 ± 3 kJ/mol are titrated between 330 and 350 mol/g. However, a higher enthalpy change is observed at higher coverages, probable due to disproportionation reactions of MMA, as described elsewhere (12). The results of MMA adsorption on H–mordenite at 473 K show a plateau corresponding to sites with enthalpy changes that vary monotonically with increasing coverage. In addition, there is an increase in apparent enthalpy change with each dose at high coverages. The number of sites titrated by MMA for H–mordenite is approximately 520 μmol/g. The average enthalpy change of adsorption for the strong sites is -219 ± 17 kJ/mol, and for the weak sites the corresponding value is -91 ± 5 kJ/mol.

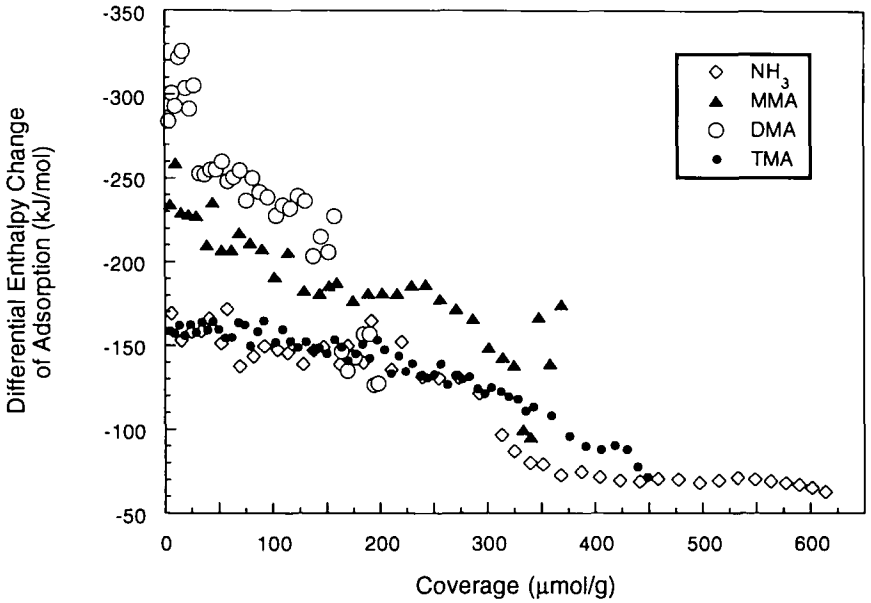

FIG. 1. Differential enthalpy changes versus coverage for adsorption of ammonia (◇), monomethylamine (▲), dimethylamine (○), and trimethylamine (●) on H–ZSM-5.

Dimethylamine Adsorption

The differential enthalpy change of DMA adsorption versus coverage on H–ZSM-5 at 473 K is very high at low coverages; however, the enthalpy change reaches a more constant value with increasing coverage, and it decreases to a lower value at high coverages. The first few points may be due to adsorption/desorption phenomena in the dosing volume of the volumetric adsorption system. The majority of the strong sites have an enthalpy change of DMA adsorption equal to -245 ± 10 kJ/mol. Weaker adsorption sites exist with an enthalpy change of DMA adsorption equal to -142 ± 13 kJ/mol. As with MMA adsorption, high enthalpy changes were observed with

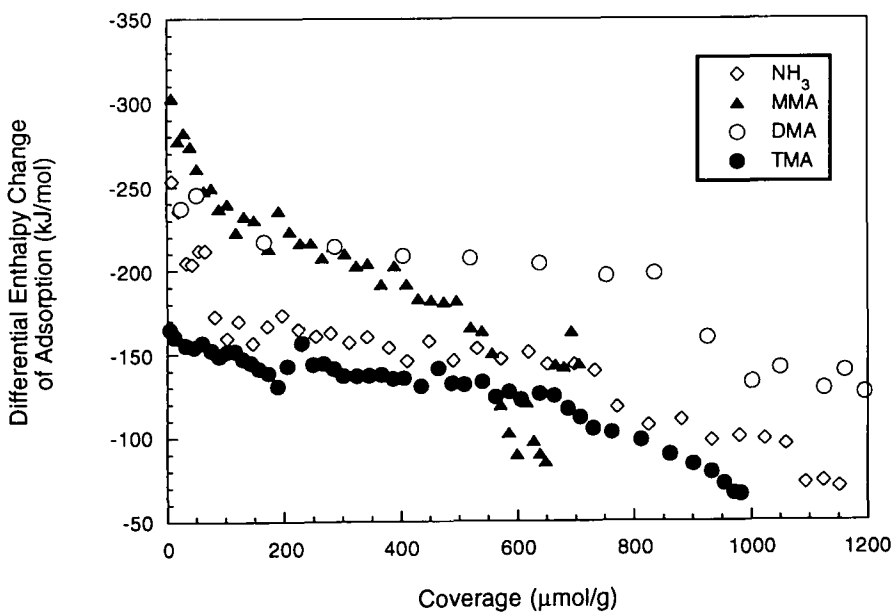

FIG. 2. Differential enthalpy changes versus coverage for adsorption of ammonia (◇), monomethylamine (▲), dimethylamine (○), and trimethylamine (●) on H–mordenite.

each dose at high coverages, probably due to disproportionation reactions (these points are not represented in the figure). The plot of differential enthalpy change versus coverage for DMA adsorption on H–mordenite at 473 K shows a gradually varying enthalpy change of adsorption, followed by titration of weak sites. The average enthalpy changes of DMA adsorption on these sites are -207 ± 8 and -134 ± 6 kJ/mol, respectively. The number of strong sites is about 900 μmol/g.

Trimethylamine Adsorption

The differential enthalpy change for TMA adsorption on H–ZSM-5 at 473 K varies gradually with increasing coverage, and the average enthalpy change of adsorption for the first 200 μmol/g of sites is -155 ± 7 kJ/mol. Weak adsorption is apparent at coverages higher than 390 μmol/g, with no apparent plateau representing weak sites. The enthalpy change of adsorption for the strongest sites is lower than for adsorption of MMA and DMA. This behavior is surprising given that TMA has the highest gas-phase proton affinity of the methylamines (see Table 1). The adsorption behavior of TMA on H–mordenite at 473 K is similar to that for TMA adsorption on H–ZSM-5. Instead of well-defined plateaus, the differential enthalpy change of adsorption decreases steadily with increasing coverage. At a coverage of approximately 700 μmol/g, the enthalpy change decreases more rapidly. The average strength of TMA adsorption on sites up to this coverage is -140 ± 12 kJ/mol. As with adsorption on H–ZSM-5, the enthalpy change of TMA adsorption on H–mordenite is lower than that for MMA or DMA. The total number of adsorption sites for TMA approaches 1000 μmol/g.

MICROCALORIMETRY OF OXYGENATES

The differential enthalpy changes of adsorption versus adsorbate coverage for dimethylether, methanol, and water on H–ZSM-5 are shown in Fig. 3. Plots of the corresponding differential enthalpy changes of adsorption versus adsorbate coverage on H–mordenite are presented in Fig. 4.

Dimethylether Adsorption

The first 10 points in Fig. 3 for the differential enthalpy change vesus coverage for dimethylether adsorption on H–ZSM-5 represent adsorption at 473 K, while the last 25 points correspond to adsorption at 373 K. Some sites have a high apparent strength, whereas a large number of sites have an intermediate enthalpy change of -91 ± 3 kJ/mol. Weak sites may also exist with an average enthalpy change of adsorption equal to -42 kJ/mol. Approximately 320 μmol/g of strong sites are titrated by DME. The differential enthalpy change of DME adsorption on H–mordenite at 373 K shows an initial region of high-strength adsorption, followed by adsorption on sites with an enthalpy change equal to -87 ± 4 kJ/mol. The enthalpy change of adsorption decreases gradually with coverage to -60 kJ/mol. The adsorption of DME titrates strong sites to a coverage of 700 μmol/g on H–mordenite.

Methanol Adsorption

The differential enthalpy change of methanol adsorption versus coverage on H–ZSM-5 at 373 K shows strong sites that adsorb methanol with an enthalpy change of -79 ± 2 kJ/mol, while the weak sites have an enthalpy change of adsorption near -66 ± 3 kJ/mol. Approximately 200 μmol/g of the stronger sites are titrated by methanol. The first 25 points in Fig. 4 for the differential enthalpy change versus coverage for methanol adsorption on H–mordenite correspond to adsorption at 473 K, while the last 8 points represent adsorption at 373 K. The enthalpy changes of adsorption on strong and weak sites are equal to -99 ± 4 and -71 ± 2 kJ/mol, respectively.

TABLE 1

Average Enthalpy Changes of Adsorption on H–ZSM-5 and H–mordenite

Base	Proton affinity PA (kJ/mol)	H–ZSM-5		H–mordenite	
		ΔH_1(kJ/mol)	ΔH_2(kJ/mol)	ΔH_1(kJ/mol)	ΔH_2(kJ/mol)
NH_3	857.7	-151 ± 11	-69 ± 3	-158 ± 8	-72 ± 2
NH_2CH_3	895.8	-204 ± 22	-98 ± 3	-219 ± 17	-91 ± 5
$NH(CH_3)_2$	922.6	-245 ± 10	-142 ± 13	-207 ± 8	-134 ± 6
$N(CH_3)_3$	938.5	-155 ± 7	-71^a	-140 ± 12	-66^a
CH_3OCH_3	807.9	-91 ± 3	-42^a	-87 ± 4	-60^a
CH_3OH	773.6	-79 ± 2	-66 ± 3	-99 ± 4	-71 ± 2
H_2O	723.8	-61 ± 3		-75 ± 3	

Note. ΔH_1 = high-strength adsorption sites; ΔH_2 = low-strength adsorption sites.

[a] Lowest measured value.

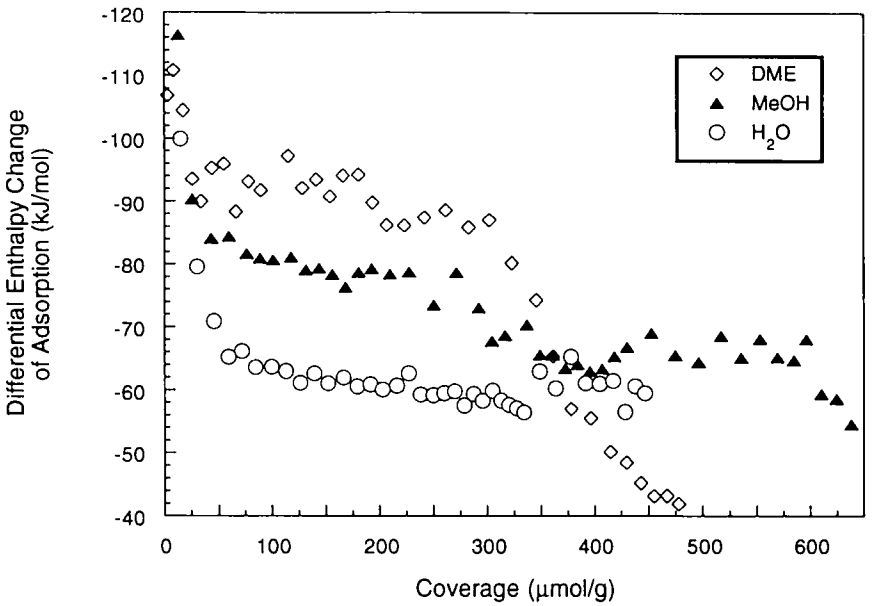

FIG. 3. Differential enthalpy changes versus coverage for adsorption of dimethylether (◇), methanol (▲), and water (○) on H–ZSM-5.

Water Adsorption

The differential enthalpy change of adsorption versus coverage of water on H–ZSM-5 at 373 K is nearly constant with respect to coverage, with the exception of several points at low coverage. The average enthalpy change of adsorption is equal to −61 ± 3 kJ/mol. The differential enthalpy change of water adsorption versus coverage on H–mordenite at 423 K shows an initial decrease in enthalpy change at low coverages, followed by a broad plateau with an average enthalpy change of adsorption equal to −75 ± 3 kJ/mol.

Coadsorption Studies

Ammonia adsorption was studied on H–mordenite following treatment with methanol. In particular, methanol adsorption at 473 K was first studied at a pressure of 5

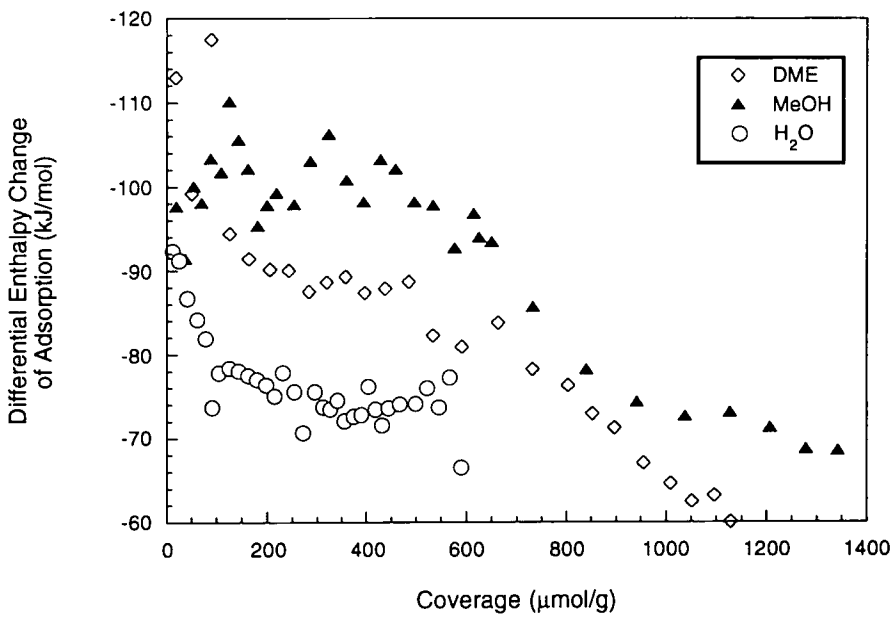

FIG. 4. Differential enthalpy changes versus coverage for adsorption of dimethylether (◇), methanol (▲), and water (○) on H–mordenite.

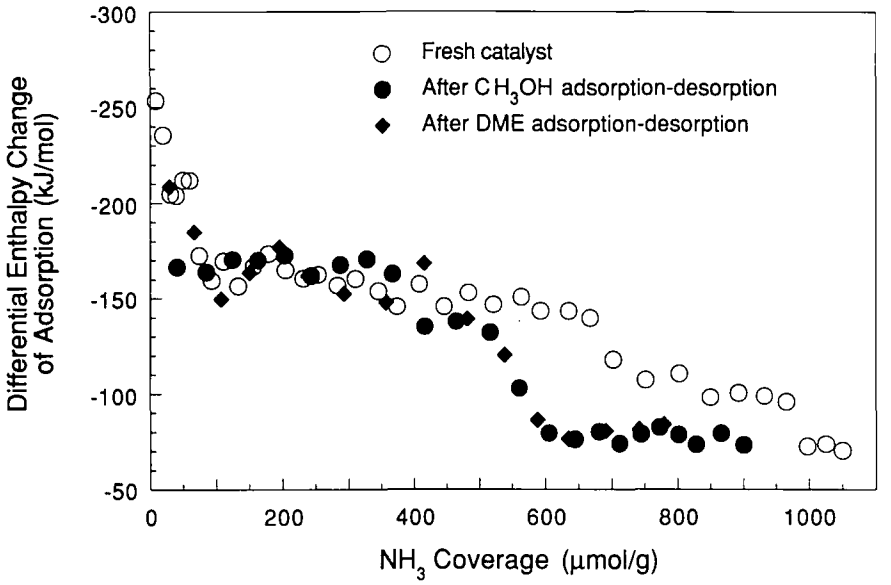

FIG. 5. Differential enthalpy change of ammonia adsorption versus coverage on H–mordenite (○) and H–mordenite with preadsorbed/desorbed methanol (●) and dimethylether (◇).

Torr, and gaseous methanol was then evacuated. The catalyst temperature was raised to 548 K, and the catalyst evacuated overnight at a pressure of 5×10^{-5} Torr. Ammonia adsorption was then conducted at 473 K. The resulting data are shown in Fig. 5, with the differential enthalpy change of ammonia adsorption versus coverage on clean H–mordenite shown for comparison. Methanol preadsorption followed by evacuation has the effect of reducing the number of strong adsorption sites. The enthalpy change of adsorption on the remaining sites is not affected by the irreverisbly bound methanol species. The effect of DME preadsorption on ammonia adsorption was similarly studied for H–mordenite. The same behavior as methanol preadsorption was apparent, as seen in Fig. 5.

INFRARED SPECTROSCOPY

Ammonia Adsorption

Infrared spectra for H–ZSM-5 have bands due to silanol and acidic hydroxyl groups at 3742 and 3612 cm^{-1}, respectively (15, 16). These bands are eliminated with adsorption of ammonia at room temperature. Increasing the desorption temperature leads first to ammonia desorption from the silanol groups, with essentially complete desorption by 573 K. Ammonia bound to acidic hydroxyl groups begins to desorb at 573 K.

Following adsorption of ammonia at room temperature, a broad band appears between 2800 and 3400 cm^{-1}, corresponding to weakly adsorbed ammonia (17), as well as strong bands at 1621 and 1493 cm^{-1}. The band at 1493 cm^{-1} corresponds to ammonium ions associated with Brønsted acid sites, while the band at 1621 cm^{-1} is most likely due to the interaction of ammonia with residual Na^+ (18–20). As gaseous ammonia is purged and the catalyst temperature is raised to 373 K, the bands due to weakly adsorbed ammonia disappear. With increasing temperature from 473 to 623 K, the intensity of the band due to ammonia adsorbed on Brønsted acid sites decreases.

Monomethylamine Adsorption

The general behavior observed in the IR spectra for monomethylamine adsorption on H–ZSM-5 at a pressure of approximately 40 Torr was similar to that for ammonia adsorption, except that the hydroxyl band due to Brønsted sites was not recovered to a significant extent upon heating in vacuum to 673 K. This behavior is consistent with the microcalorimetric result that MMA adsorbs more strongly than NH_3.

Figure 6 shows infrared spectra (a) after MMA adsorption at room temperature and after purging in flowing He at 298, 373, 473, 573, and 673 K (spectra (b)–(f), respectively). With gaseous MMA present, weakly adsorbed MMA gives rise to a broad series of bands from 2600 to 3200 cm^{-1}. The strong bands at 1597 and 1464 cm^{-1} are similar in position to the asymmetric and symmetric vibrations measured by Ghosh and Curthoys for MMA adsorbed on Brønsted acid sites of H–mordenite (20). The band at 1597 cm^{-1} overlaps with MMA adsorbed on Lewis acid sites, and the coordination of MMA with Na^+ cations could not be determined (20, 21). The presence of these two bands at high temperatures indicates that MMA is strongly adsorbed on the Brønsted acid sites.

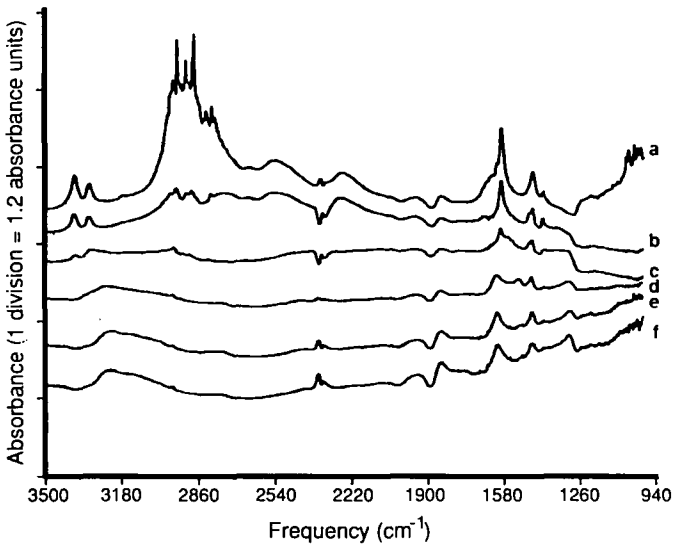

FIG. 6. Infrared spectra for (a) MMA adsorption at 40 Torr and room temperature, (b) after purging with He at room temperature, (c) 373 K, (d) 473 K, (e) 523 K, and (f) 673 K.

Methanol Adsorption

Figure 7 shows IR spectra ratioed to the clean zeolite as background to monitor the absorption bands of methanol on H–ZSM-5 after (a) methanol adsorption at 7 Torr and 298 K and after purging in flowing He at 298, 373, 473, 523, 573, and 623 K (spectra (b)–(g), respectively). Room-temperature adsorption of methanol results in a broad band with peaks at 2949 and 2842 cm^{-1} and shoulders at 2989 at 2922 cm^{-1}. These peaks are due to the O–H stretch of hydrogen-bound methanol (15). Purging with He and raising the temperature to 523 K results in elimination of all bands except those at 2990, 2957, and 2856 cm^{-1}. The peak at 2856 cm^{-1} can be assigned to the symmetric CH_3 vibration of methoxyl groups resulting from methyl substitution at Brønsted acid sites; the accompanying band at 2957 cm^{-1} results from the asymmetric CH_3 vibration (15, 22, 23). The peak locations and shapes agree with those of Kubelkova *et al.*, who measured 2850 and 2952 cm^{-1} for the symmetric and antisymmetric vibrations for methoxyl species on H–ZSM-5 (15).

In Situ Methylamine Synthesis

Figure 8 shows the C–H and N–H stretching spectral region after calcination and exposure to a flowing gas mixture of methanol and ammonia at 298, 373, 473, 523, 573, 623, and 673 K (spectra (a)–(g), respectively). The bands at 2922 and 2989 cm^{-1} disappear at temperatures above 373 K, leaving the pair of methoxyl bands at 2957 and 2855 cm^{-1}. The concentration of methoxyl species remains low and relatively unchanged as the reaction temperature is raised from 473 to 673 K.

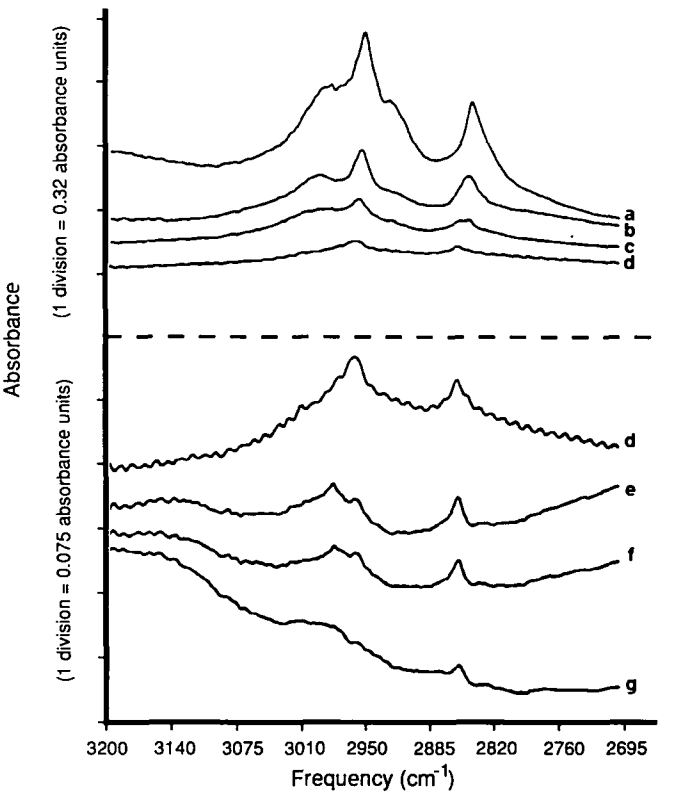

FIG. 7. Infrared spectra for (a) CH_3OH adsorption at 7 Torr and room temperature, (b) after purging with He at room temperature, (c) 373 K, (d) 473 K, (e) 523 K, (f) 573 K, and (g) 623 K.

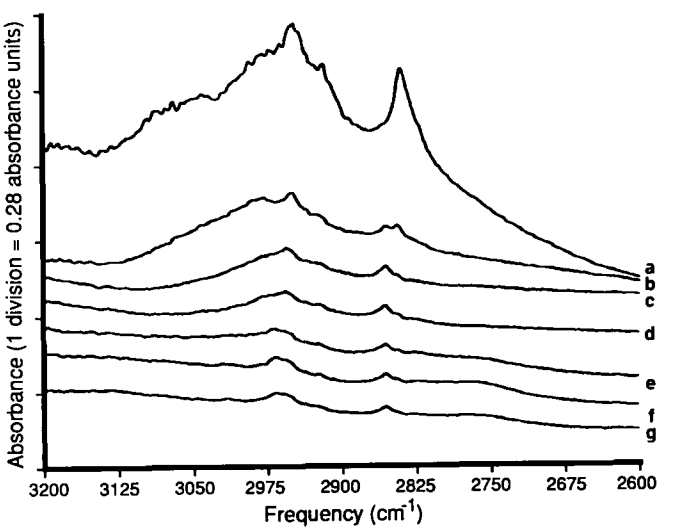

FIG. 8. Infrared spectra of methanol region for H–ZSM-5 in a flowing mixture of CH_3OH (10 Torr) and NH_3 (7 Torr) at (a) 298 K, (b) 373 K, (c) 473 K, (d) 523 K, (e) 573 K, (f) 623 K, and (g) 673 K.

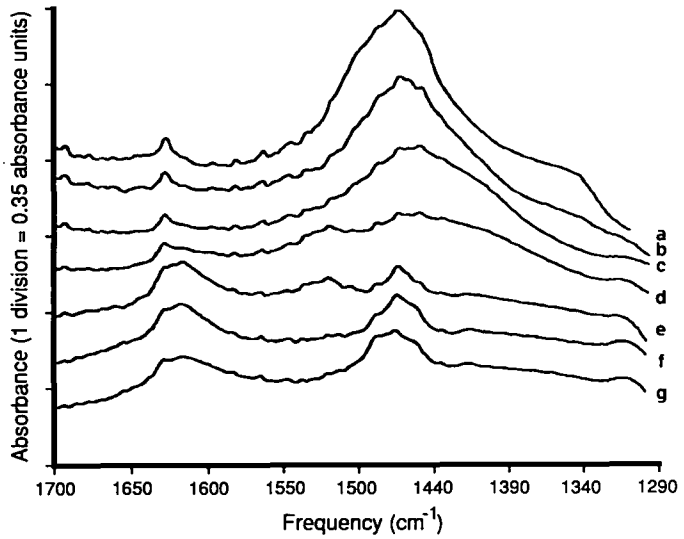

FIG. 9. Infrared spectra of NH_3 and MMA regions for H–ZSM-5 in a flowing mixture of CH_3OH (10 Torr) and NH_3 (7 Torr) at (a) 298 K, (b) 373 K, (c) 473 K, (d) 523 K, (e) 573 K, (f) 623 K, and (g) 673 K.

The N–H deformation region is shown in Fig. 9, with the H–SZM-5 sample under the methylamine synthesis conditions of Fig. 8. The peak centered at 1469 cm^{-1} is most likely due to ammonia adsorbed on Brønsted acid sites. A second weak peak at 1625 cm^{-1} can be assigned to ammonia adsorbed at Na^+ cations (weak Lewis sites). Increasing the reaction temperature from 373 to 523 K results in decreasing amounts of adsorbed ammonia. At 573 K, two bands appear at 1611 and 1465 cm^{-1} that can be assigned to adsorbed MMA. The MMA bands grow with increasing temperature, corresponding to increased product formation. Importantly, the band at 3612 cm^{-1} due to acidic hydroxyl species is absent under reaction conditions at 673 K, indicating that the Brønsted acid sites become largely covered by ammonia and methylamines in gas mixtures of methanol and ammonia typically used for methylamine synthesis. Under these reaction conditions, neither catalyst showed deactivation which would indicate coke formation (12).

DISCUSSION

Thermodynamics of Adsorption Processes

Table 1 summarizes the proton affinities and enthalpy changes of adsorption for the reactants and products of methylamine synthesis. A plot of the enthalpy change of adsorption versus proton affinity for the various bases on ZSM-5 and mordenite is shown in Fig. 10. In general, molecules with a higher proton affinity have a higher enthalpy change of adsorption, in accord with previous results over amorphous silica–alumina (4). The enthalpy change of adsorption varies nearly linearly with proton affinity for dimethylether, ammonia, monomethylamine, and dimethylamine. This linear correlation is consistent with the fact that these bases are present as positively charged species in the zeolite micropore structure. Accordingly, the interaction of these bases with the catalyst

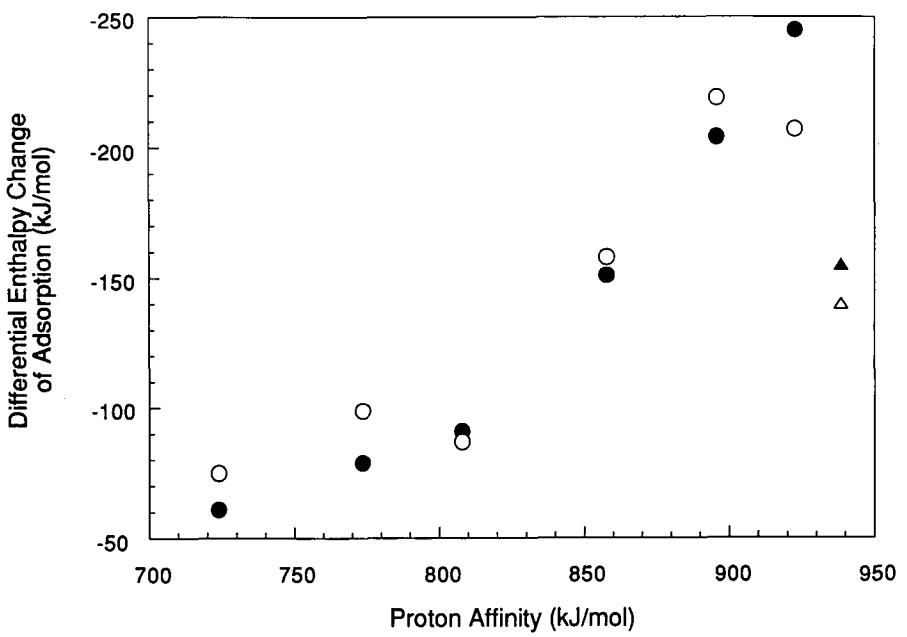

FIG. 10. Average enthalpy change of adsorption of various bases versus proton affinity for Brønsted acid sites of H–ZSM-5 (●) and H–mordenite (○). Triangles represent data for trimethylamine adsorption.

is dominated by the transfer of a proton from the zeolite lattice to the basic acceptor. Trimethylamine is a strong base that shows a notable exception to the linear correlation of enthalpy change of adsorption versus proton affinity. This result may be due to steric effects within the micropores of the zeolite, since the enthalpy change of TMA adsorption did not show such anomalous behavior with respect to proton affinity on amorphous silica–alumina (4).

In contrast to the aforementioned behavior of the strong bases, the enthalpy change of adsorption is not strongly dependent on proton affinity for the weaker bases, water and methanol. These results suggest that the interaction of these bases with the catalyst contains significant contributions from nonspecific interactions, such as van der Waals interactions. These nonspecific interactions lead to enthalpy changes of adsorption that are typically from −30 to −70 kJ/mol, depending on the polarizibility of the adsorbate molecule. Thus, the magnitude of these interactions is comparable to the magnitude of the total enthalpy change of adsorption for water and methanol, and the enthalpy change of adsorption is expected to be a weak function of the proton affinity. In general, the heat of adsorption will reflect contributions from both electrostatic and dispersive interactions. Zeolite structure, in particular the geometry around the acid site, will influence both of these interactions through the size and shape of the adsorbate.

Ammonia has a higher enthalpy change of adsorption than methanol and may be expected to be the dominant species adsorbed on the Brønsted acid sites in the presence of these two gases. Monomethylamine, the primary reaction product at low conversion, has a higher enthalpy change of adsorption than ammonia; therefore, MMA may also occupy a significant fraction of the adsorption sites under reaction conditions. Infrared spectra collected with the H–ZSM-5 sample under methylamine synthesis conditions confirm that the Brønsted acid sites are coordinated to a significant extent with adsorbed amine species.

Methanol can coordinate with Brønsted acid sites and transform Brønsted hydroxyl groups into methoxyl groups. Most of the early work on alkoxyl formation has been performed with amorphous solid acids. Among the catalysts showing alkoxyl formation are alumina (24–28), Cu/ZnO (29), ZnO (30), TiO_2 (31, 32), MgO (33), Fe_2O_3 (34), and Cr_2O_3 (35). The adsorption of methanol on zeolites has also been the subject of spectroscopic investigations. Bosacek and Tvaruzkova demonstrated the existence of a weakly held form of methanol and a strongly held form present as methoxyl groups on H–X zeolite (22). Salvador and Kladnig performed a similar IR study of methanol adsorption on H–Y zeolites (23), and the results were essentially the same as those of Bosacek and Tvaruzkova. Derouane *et al.* (36) used ^{13}C NMR to show that methoxyl species led to the formation of dimethylether during dehydration of methanol on NaGe-X. Ison and Gorte conducted TPD and IR studies and concluded that methanol has two adsorption states on H–ZSM-5 (37). Subsequent studies by the same group cited alkoxyl formation on the acid sites (38–40).

A recent study by Kubelkova *et al.* suggests the existence of several adsorption states for methanol on H–Y and H–ZSM-5 zeolites (15). At room temperature, methanol was present as hydrogen-bonded species and as methyl carboxonium ions ($CH_3OH_2^+$) on both catalysts. At temperatures from 373 to 453 K, methoxyl groups predominated on the zeolite, while the methoxyl groups were converted to DME at higher temperatures.

The low enthalpy changes observed in the present study for adsorption of CH_3OH and DME on H–ZSM-5 and H–mordenite indicate that methoxyl species are not particularly stable in comparison to NH_3 adsorbed on Brønsted acid sites. The results in Fig. 5 of the coadsorption experiments indicate that methoxyl species apparently block sites for strong ammonia adsorption. Furthermore, these methoxyl species do not appear to react with ammonia at a significant rate at 473 K.

Implications of Results for Methylamine Synthesis

The microcalorimetric and IR spectroscopic results of the present study provide valuable information about the thermodynamic and chemical aspects of methylamine synthesis reactions over H–ZSM-5 and H–mordenite. The quantitative aspects of these catalytic cycles in methylamine synthesis reactions will be addressed elsewhere in greater detail (12). However, the general features of the reactive intermediates involved in these reactions will be outlined below.

The reactivity of methoxyl species in methylamine synthesis reactions has not been studied in the literature. These species predominate on the surface under conditions of flowing methanol at elevated temperatures. These are conditions for which methanol is converted to dimethylether and water. Accordingly, methoxyl species may be reactive intermediates in DME formation over H–ZSM-5 and H–mordenite.

The rate of methoxyl formation has been related to acid strength in the literature (23). More labile protons of hydroxyl groups form methoxyl species more easily. Similarly, if a proton is replaced by a methyl group on an acid site, then the C–O bond (corresponding to the original H–O bond) may be weaker for a more acidic site. Thus, the methyl group substituted at a strong acid site may react more rapidly with a nucleophile such as methanol. This possibility is intriguing in light of quantum chemical calculations of Kazansky and Senchenya (41) which showed that the activation energy for the transition from

alkoxyl to carbenium ion-like species (i.e., an alkoxyl species with high C–O bond polarization) would be on the order of 10–15 kcal/mol, a value that is comparable to the overall activation energy for the formation of DME from methanol (12).

The microcalorimetric results indicate that all of the nitrogen-containing bases are adsorbed on the Brønsted acid sites considerably more strongly than methanol and DME, and MMA and DMA are adsorbed more strongly than ammonia. Therefore, it is possible that methoxyl species are not reactive intermediates in the formation of MMA, DMA, and TMA from methanol and ammonia, i.e., methoxyl species participate in DME production from methanol but do not participate in methylamine formation. In agreement with this suggestion is the observation from *in situ* IR studies that the surface concentration of methoxyl species is low under methylamine synthesis conditions.

The *in situ* IR experiments indicate that the ammonia coverage is low on the catalyst surface during methylamine synthesis conditions. This result is consistent with the first-order dependence of reaction rate on ammonia pressure (12). The coverage by methylamines increases as temperature increases from 573 to 673 K, and this is the temperature range in which the rate of methylamine synthesis becomes significant. Furthermore, the *in situ* IR studies show that the Brønsted acid sites become largely covered by methylamines under reaction conditions. This result is in agreement with the microcalorimetric result that the enthalpy changes of adsorption of MMA and DMA are significantly larger than the enthalpy change of ammonia adsorption.

If the Brønsted acid sites are essentially fully covered by adsorbed amine species, as suggested by our microcalorimetric and IR studies, then the addition of methyl groups to adsorbed amines in methylamine synthesis may take place via methylamine disproportionation reactions and/or reaction of adsorbed amines with gaseous or weakly adsorbed methanol or DME. Evidence for the occurrence of these disproportionation reactions is provided by the present calorimetric studies that show high apparent enthalpy changes of adsorption for MMA and DMA at conditions for which the pressures of these amines become significant. These disproportionation processes apparently involve reactions of strongly adsorbed amines with gaseous or weakly adsorbed species present at these higher pressures.

CONCLUSIONS

Microcalorimetric measurements have determined the enthalpy changes of adsorption on H–ZSM-5 and H–mordenite of methanol, dimethylether, water, ammonia, monomethylamine, dimethylamine, and trimethylamine. These species are the various constituents of methylamine synthesis reactions. Higher enthalpy changes of adsorption are observed for molecules with higher proton affinities, trimethylamine being the notable exception. Methanol adsorption leads to the formation of methoxyl groups. Ammonia and methylamines adsorb on Brønsted acid sites to form positively charged ammonium species. *In situ* IR studies indicate that while methoxyl species predominate on the surface with the catalyst under flowing methanol, the Brønsted acid sites become largely covered by ammonia and methylamines under methylamine reaction conditions. The combination of these microcalorimetric and IR spectroscopic studies suggests that methoxyl species may be reactive intermediates in dimethylether formation from methanol; however, the formation of methylamines from methanol and ammonia most likely takes place via positively charged ammonium species.

ACKNOWLEDGMENTS

This work was supported by the Department of Energy and through a Joint China–U.S. Cooperative Research Grant administered by the National Science Foundation. One of us (DTC) thanks the National Science Foundation for a graduate fellowship. We also thank Randy Cortright and Jeff Kobe at the Univesity of Wisconsin for valuable insight during the latter stages of this project.

REFERENCES

1. Heilen, G., Mercker, H. J., Frank D., Reck, R. A. and Jaeckh, R., *in* "Ullman's Encyclopedia of Industrial Chemistry, 5th ed." (W. Gerhartz, Ed.), p. 1. VCH Verlagsgesellschaft, Weinheim, 1987.
2. Baiker, A., *in* "Heterogeneous Catalysis and Fine Chemicals: Proceedings of an International Symposium, Poitiers, France, March 15–17, 1988" (M. Guisnet and J. Berrault, Eds.), p. 238. Studies in Surface Science and Catalysis, No. 41, Elsevier, Amsterdam, 1988.
3. Weigert, F. J., *J. Catal.* **103,** 20 (1987).
4. Cardona-Martinez, N., and Dumesic, J., *J. Catal.* **128,** 23 (1991).
5. Kapustin, G. I., Kustov, L. M., Glonti, G. O., Brueva, T. R., Borovkov, V. Y., Klyachko, A. L., Rubinstein, A. M., and Kazanskii, V. B., *Kinet. Katal.* **25,** 1129 (1984).
6. Avgul, N. N., Kiselev, A. V., Kurdyukova, L. Y., and Serdobov, M. V. *Russ. J. Phys. Chem.* **42,** 96 (1968).
7. Earl, W. L., Fritz, P. O., Gibson, A. A. V. and Lunsford, J. H., *J. Phys. Chem.* **91,** 2091 (1987).
8. Meinhold, R. H., Parker, L. M., and Bibby, D. M., *Zeolites* **6,** 491 (1986).
9. Morishige, K., Kittaka, S., and Takao, S., *J. Chem. Soc. Faraday Trans. 1* **80,** 993 (1984).
10. Benerak, L. and Kraus, M., *in* "Comprehensive Chemical Kinetics" (C. Banford and C. Tipper, Eds.), Chap. 3. Elsevier, New York, 1978.
11. Chang, C., *Catal. Rev.-Sci. Eng.* **25,** 1 (1983).
12. Chen, D., Zhang, L., Kobe, J., Cortright, R., Chen, Y., and Dumesic, J. A., in preparation.
13. Cardona-Martinez, N., and Dumesic, J. A., *J. Catal.* **125,** 427 (1990).
14. Chen, D., Sharma, S., Filimonov, I., and Dumesic, J., *Catal. Lett.* **12,** 201 (1992).

15. Kubelkova, L., Novakova, J., and Nedomova, K., *J. Catal.* **124,** 441 (1990).
16. Ono, Y., and Mori, T., *J. Chem. Soc. Faraday Trans. I* **77,** 2209 (1981).
17. Dines, T., Rochester, C., and Ward, A., *J. Chem. Soc. Faraday Trans. I* **87,** 1611 (1991).
18. Ward, J., *in* "Zeolite Chemistry and Catalysis" (J. Rabo, Ed.), p. 118. American Chemical Society, New York, 1976.
19. Ward, J., *J. Catal.* **11,** 251 (1968).
20. Ghosh, A., and Curthoys, G., *J. Chem. Soc. Faraday Trans. I* **80,** 99 (1984).
21. Jobson, E., Baiker, A., and Wokaun, A., *J. Chem. Soc. Faraday Trans. I* **86,** 1131 (1990).
22. Bosacek, V., and Tvaruzkova, Z., *Collect. Czech. Chem. Commun.* **36,** 551 (1971).
23. Salvador, P., and Kladnig, W., *J. Chem. Soc. Faraday Trans. I* **73,** 1153 (1977).
24. Greenler, R. G., *J. Chem. Phys.* **37,** 2094 (1962).
25. Naito, K., *Bull. Osaka Ind. Res. Inst.* **10,** 160 (1959).
26. Arai, H., Saito, Y., and Yoneda, Y., *Bull. Chem. Soc. Jpn.* **40,** 731 (1967).
27. Deo, A. V., and Dalla Lana, I. G., *J. Phys. Chem.* **73,** 716 (1969).
28. Deo, A. V., Chuang, T. T., and Dalla Lana, I. G., *J. Phys. Chem.* **75,** 234 (1971).
29. Edwards, J. F., and Schrader, G. L., *J. Phys. Chem.* **89,** 782 (1985).
30. Koga, O., Onishi, T., and Tamaru, K., *J. Chem. Soc. Faraday Trans. I* **76,** 19 (1980).
31. Miyata, H., Nakajima, T., and Kubokawa, Y., *J. Catal.* **69,** 292 (1981).
32. Rossi, O. F., Busca, G., Lorenzelli, V., Saur, O., and Lavalley, J. C., Langmuir **3,** 52 (1987).
33. Liang, S., and Gay, I., *Langmuir* **1,** 593 (1985).
34. Zaki, M. I., and Sheppard, N., *J. Catal.* **80,** 114 (1983).
35. Osipova, N. A., Davydov, A. A., Kurina, L. N., and Loiko, V. E., *Zh. Fiz. Khim.* **59,** 1479 (1985).
36. Derouane, E., Dejaifve, P., and Nagy, J., *J. Mol. Catal.* **3,** 453 (1977).
37. Ison, A., and Gorte, R. J., *J. Catal.* **89,** 150 (1984).
38. Grady, M. C., and Gorte, R. J., *J. Phys. Chem.* **89,** 1305 (1985).
39. Aronson, M. T., Gorte, R. J., and Farneth, W. E., *J. Catal.* **98,** 434 (1986).
40. Aronson, M. T., Gorte, R. J., and Farneth, W. E., *J. Catal.* **105,** 455 (1987).
41. Kazansky, V. B., and Senchenya, I. N., *J. Catal.* **119,** 108 (1989).